Strasbourg (France)

MANUSCRIPT COVER PAGE FORM

E-MRS Symposium : D

Paper number : #2037

Title of paper : COMPREHENSIVE MODELING OF ION-IMPLANT AMORPHIZATION IN SILICON.

Corresponding author : K. R. C. Mok

Full Mailing Address : Caroline Mok. Dpto. Electronica. Universidad de Valladolid. E.T.S.I.T. Campus Miguel Delibes S/N. 47011. Valladolid. Spain.

Telephone : +34 983 42 30 00 ext 5510

Fax : +34 983 42 36 75

E-mail : g0202446@nus.edu.sg

Comprehensive modeling of ion-implant amorphization in silicon

K. R. C. Mok,[1,2] M. Jaraiz,[1] I. Martin-Bragado,[1,3] J. E. Rubio,[1]
P. Castrillo,[1] R. Pinacho,[1] M. P. Srinivasan,[2] and F. Benistant[4]

[1] *Departamento de E. y Electrónica,*
Universidad de Valladolid. ETSIT Campus Miguel Delibes, 47011 Valladolid, Spain

[2] *Department of Chemical & Biomolecular Engineering,*
National University of Singapore. 4 Engineering Drive 4, Singapore 117576

[3] *Synopsys. Karl-Hammerschmidt Strasse 34,*
D-85609 Aschheim/Dornach, Germany

[4] *Chartered Semiconductor Manufacturing. 60 Woodlands*
Industrial Park D, Street 2, Singapore 738406.

Abstract

A physically based model has been developed to simulate the ion-implant induced damage accumulation up to amorphization in silicon. Based on damage structures known as amorphous pockets (AP), which are three-dimensional, irregularly shaped agglomerates of interstitials (I) and vacancies (V) surrounded by crystalline silicon, the model is able to reproduce a wide range of experimental observations of damage accumulation and amorphization with interdependent implantation parameters. Instead of recrystallizing the I's and V's instantaneously, the recrystallization rate of an AP containing nI and mV is a function of its effective size, defined as min(n, m), irrespective of its internal spatial configuration. The parameters used in the model were calibrated using the experimental silicon amorphous-crystalline transition temperature as a function of dose rate for C, Si, and Ge. The model is able to show the superlinear damage build-up with dose, the extent of amorphous layer and the superadditivity effect of polyatomic ions.

I. INTRODUCTION

Ion implantation is a well-established processing technique, widely used in integrated circuits fabrication for purposes such as the controlled doping of silicon and for pre-amorphization implants. However, it inevitably leads to damage generation, which has to be subsequently removed by annealing. Modeling and prediction of ion-implant induced damage accumulation in silicon is crucial to the simulation of silicon processing. Upon annealing, the damage contributes to dopant clustering and results in transient enhanced diffusion, which can only be predicted with an accurate damage accumulation model. Futhermore, it is important to predict the extent of amorphization as it impacts the ion-channeling of subsequent implants and the implant damage evolution during anneals.

However, modeling of damage accumulation in semiconductors is difficult due to the diversity of damage types induced by ion-implantation and the many interdependent implantation parameters like ion mass, dose, dose rate and substrate temperature. Damage accumulation from implant cascades is a competition between damage generation and dynamic annealing depending on the implantation parameters. An increase in dose rate increases the rate of generation, while higher substrate temperature increases the rate of recombination/recrystallization of defects. An atomistic model [1, 2] that is able to reproduce the amorphous-crystalline transtion temperatures and the regrowth behavior in silicon has earlier been proposed. In that model, based on the interstitial-vacancy (IV) pair as an elementary unit, the recombination rate of an IV pair decreases as the number of neighboring IV pairs increases.

II. OUR MODEL

In this work, we introduce a model, based on the damage structures known as amorphous pockets (AP, [3]), which reproduces the amorphous-crystalline transition temperature for C, Si and Ge ion implants. The coordinates of the ion-implantation induced Frenkel pairs obtained from the binary collision program [4] are inserted, cascade after cascade, into an atomistic non-lattice kinetic Monte Carlo simulator [5]. Instead of undergoing immediate recrystallization, interstitials (I) and vacancies (V) are assumed to form a distinct, disordered region (AP) when they are within a capture distance (second neighbor distance) of each

other. An AP is, therefore, a three-dimensional, irregularly shaped agglomerate of I's and V's surrounded by crystalline silicon. Here, the I and V terms are used as a means of referring (for an I_nV_m AP) to a disordered region of a volume size roughly equal to nI+mV with a net excess or deficit of atoms n-m. These damage structures are in direct correspondence to the APs studied by molecular dynamics (MD) [3, 6], produced from single cascades in Si. Recrystallization of the APs by annealing in MD studies indicates that larger pockets have greater stability against recrystallization, as evidenced by their larger effective activation energies. In our approach, the AP recrystallization rate (shrinkage rate) is characterized by the effective size of the AP, s=min(n, m). In this model, an AP of size s is assumed to shrink to $(s-1)$ at a rate given by $\alpha s^{\beta}\exp(-E_{\mathrm{act}}(s)/kT)$. The activation energy for recrystallization (corresponding to the *apparent* activation energy mentioned in Ref. [3]) is assumed to be a function of s alone, irrespective of the internal spatial configuration. The APs can shrink (dynamic annealing) if the temperature is high enough, or they can grow by incorporating extra I's or V's as the implant proceeds. In this model, pure interstitials (I_nV_0) and vacancy clusters (I_0V_m) are considered to be subsets of the APs, with their own characteristic emission rates [7, 8]. Once an AP with a net excess of I's or V's has completely recrystallized, the remaining I's or V's behave as pure clusters. Similarly, during subsequent implant, if a defect of the opposite type is within its capture radius, pure clusters can transform back into an I_nV_m AP and have a chance of recrystallizing. This allows for a self-consistent treatment of pure clusters and APs (I_nV_m).

In this model, the accumulation of APs (as well as point defects and pure clusters) gives rise to locally, fully amorphized regions when the defect concentration (I+V) reaches the amorphization threshold, taken to be $1.5\times10^{22}\,\mathrm{cm}^{-3}$ (30 % Si atomic concentration). With this threshold, we correctly reproduce the critical doses for amorphization for B, P and Sb implants at low temperature (100 K) [9], where the effect of dynamic annealing can be neglected.

III. SIMULATION RESULTS

We have used the experimental data from Ref. [10] to determine α, β and E_{act}(s). The experimental data corresponds to the amorphous-crystalline transition temperatures, as a function of dose rate, for (100) silicon irradiated with 80 keV ions to a dose of 1 $\times$

$10^{15}\,\text{cm}^{-2}$ for Si and Ge, and $2 \times 10^{15}\,\text{cm}^{-2}$ for C. As seen in Fig. 1, the model is able to very accurately reproduce all the experimental data for different ion mass, dose rate and implant temperature. In the simulations, following the experimental criteria, the transition temperatures were determined as the highest implant temperature that produced a buried amorphous layer. Figure 1 shows the best-fit lines obtained from simulations for each ion. The experimentally determined activation energies for C, Si and Ge are 0.70 eV, 0.79 eV and 1.11 eV respectively [10].

The single set of parameters used is α=$5\times10^{-4}\,\text{cm}^2\text{s}^{-1}$, β=0.66 and $E_{\text{act}}(\text{s})=0.67+0.024s$, up to a maximum of 2.7 eV, which is the activation energy of recrystallization for a planar amorphous-crystalline interface of a fully amorphized region [11]. For each ion, the size s corresponding to its characteristic activation energy could be interpreted as potentially being the dominant or controlling AP size, larger for heavier ions as expected. If the $E_{\text{act}}(\text{s})$ function is replaced with a step-wise function ($E_{\text{act}}(\text{s})$=2.7 eV) beyond a given size, all ions with smaller characteristic sizes continue to yield the same simulated amorphous-crystalline transition temperature. Therefore, the $E_{\text{act}}(\text{s})$ given above can so far only be said to be valid up to the characteristic energy or size of Ge.

Besides reproducing the amorphous-crystalline transtion temperatures, the model is able to simulate a diversity of experiments. The superlinear damage accumulation with dose [12, 13] can be seen from Fig. 2, for 80 keV Si and Ge implants at room temperature and a dose rate of $5 \times 10^{12}\,\text{cm}^{-2}\text{s}^{-1}$. 100 % total damage represents a continuous amorphous layer in the simulations. At the initial low implant dose, damage is relatively dilute and there is substantial recrystallization of the smaller APs. As dose increases, cascades overlap and the larger, more stable APs are not readily recrystallized, resulting in a superlinear increase in damage. The damage subsequently saturates when an amorphous layer is formed.

Figure 3 shows the normalized total damage as a function of implant temperature as obtained from simulations. Damage decreases with increase in implant temperature, due to the higher rate of dynamic annealing. Being consistent with experimental observations [14], the decrease in damage is steeper for lighter ions than for heavier ions, as the damage generated by lighter ions are more dilute, with smaller APs, while the APs generated by heavier ions are extended towards larger sizes.

The extent of the amorphous layer is important as it affects subsequent damage evolution and dopant diffusion. The depth of the amorphous layer for a 100 keV, $1\times10^{15}\,\text{cm}^2$ Si implant

at room temperature through a 25 nm oxide layer has been experimentally determined to be 186 nm [15]. The same amorphized depth was obtained in our simulation under the same conditions using a dose rate of $1 \times 10^{12}\,\mathrm{cm^{-2}s^{-1}}$. In the case of Si implants, the critical temperature for amorphization is close to room temperature, implying that amorphizing implants would be sensitive to changes in temperature or dose rate. Our simulations show that at this implant temperature, the change in depth of the amorphous layer is $\pm 10\,\%$, over an order of magnitude of change in dose rate ($1 \times 10^{11}\,\mathrm{cm^{-2}s^{-1}}$ to $1 \times 10^{13}\,\mathrm{cm^{-2}s^{-1}}$). This magnitude of change in dose rate is estimated to correspond to a $\pm 25\,^{\circ}\mathrm{C}$ change in implant temperature [10].

Implanting polyatomic clusters instead of individual atoms, for example C_n [16] and decaborane [17], has been experimentally observed to result in more damage, also known as the superadditivity effect. Implant simulations at room temperature of C and C_6 at an atomic dose of $5 \times 10^{13}\,\mathrm{cm^{-2}}$, results in 10 % more damage by using C_6 instead of C.

IV. CONCLUSIONS

In conclusion, a physical model of damage accumulation up to amorphization in silicon has been developed. It is based on the assumption that the recrystallization rate of APs is only a function of their size. This model accounts for the contribution to damage from point defects, APs and pure clusters. Despite its conceptual simplicity, the model is able to show experimentally observed ion mass, dose and temperature dependent effects.

References

---

[1] L. Pelaz, L. A. Marques, M. Aboy, J. Barbolla, and G. H. Gilmer, Appl. Phys. Lett. **82**, 2038 (2003).

[2] L. A. Marques, L. Pelaz, M. Aboy, L. Enriquez, and J. Barbolla, Phys. Rev. Lett. **91**, 135504 (2003).

[3] M. J. Caturla, T. Diaz de la Rubia, L. A. Marques, and G. H. Gilmer, Phys. Rev. B **54**, 16683 (1996).

[4] M. T. Robinson, Phys. Rev. B **40**, 10717 (1989).

[5] M. Jaraiz, P. Castrillo, R. Pinacho, I. Martin-Bragado, and J. Barbolla, in *Simulation of Semiconductor Processes and Devices 2001*, edited by D. Tsoukalas and C. Tsamis (Springer-Verlag, Vienna, 2001), pp. 10–17.

[6] K. Nordlund, M. Ghaly, R. S. Averback, M. Caturla, T. Diaz de la Rubia, and J. Tarus, Phys. Rev. B **57**, 7556 (1998).

[7] N. E. B. Cowern, G. Mannino, P. A. Stolk, F. Roozeboom, H. G. A. Huizing, J. G. M. van Berkum, F. Cristiano, A. Claverie, and M. Jaraiz, Phys. Rev. Lett. **82**, 4460 (1999).

[8] A. Bongiorno, L. Colombo, and T. Diaz de la Rubia, Europhys. Lett. **43**, 695 (1998).

[9] F. F. Morehead, B. L. Crowder, and R. S. Title, J. Appl. Phys. **43**, 1112 (1972).

[10] R. D. Goldberg, J. S. Williams, and R. G. Elliman, Nucl. Instrum. Meth. B **106**, 242 (1995).

[11] K. A. Jackson, J. Mater. Res. **3**, 1218 (1988).

[12] O. W. Holland, S. J. Pennycook, and G. L. Albert, Appl. Phys. Lett. **55**, 2503 (1989).

[13] G. Bai and M.-A. Nicolet, J. Appl. Phys **70**, 649 (1991).

[14] G. Hobler and G. Otto, Materials Science in Semiconductor Processing **6**, 1 (2003).

[15] H. Cerva and G. Hobler, J. Electrochem. Soc. **139**, 3631 (1992).

[16] J. A. Davies, G. Foti, L. M. Howe, J. B. Mitchell, and K. B. Winterbon, Phys. Rev. Lett. **34**, 1441 (1975).

[17] J. Matsuo, T. Aoki, K. ichi Goto, T. Sugii, and I. Yamada, in *Mat. Res. Soc. Symp. Proc.* (MRS, 1998), vol. 532, pp. 17–22.

List of figure captions

FIG 1. Simulation (lines) compared to experimental data (open symbols, from Ref. [10]) for amorphous-crystalline transition temperatures as a function of dose rate, for (100) silicon irradiated with 80 keV ions to a dose of $1 \times 10^{15}\,\mathrm{cm}^{-2}$ for Si and Ge, and $2 \times 10^{15}\,\mathrm{cm}^{-2}$ for C.

FIG 2. Superlinear damage accumulation with dose for 80 keV Si and Ge implants at room temperature and a dose rate of $5 \times 10^{12}\,\mathrm{cm}^{-2}\mathrm{s}^{-1}$.

FIG 3. Normalized total damage as a function of implant temperature as obtained from simulations, for silicon irradiated with 80 keV ions to a dose of $1 \times 10^{15}\,\mathrm{cm}^{-2}$ for Si and Ge, and $2 \times 10^{15}\,\mathrm{cm}^{-2}$ for C.

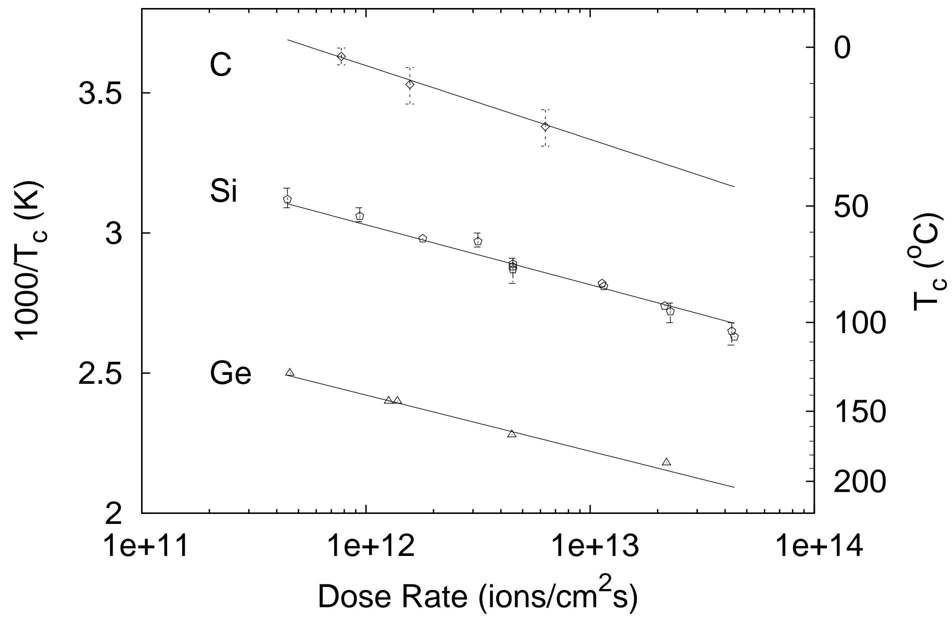

FIG. 1:

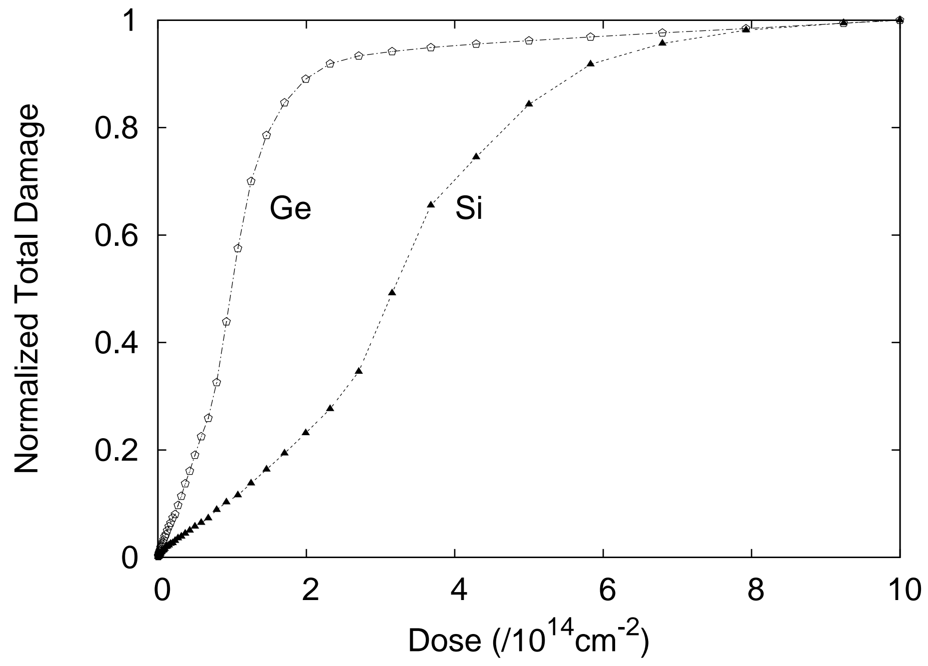

FIG. 2:

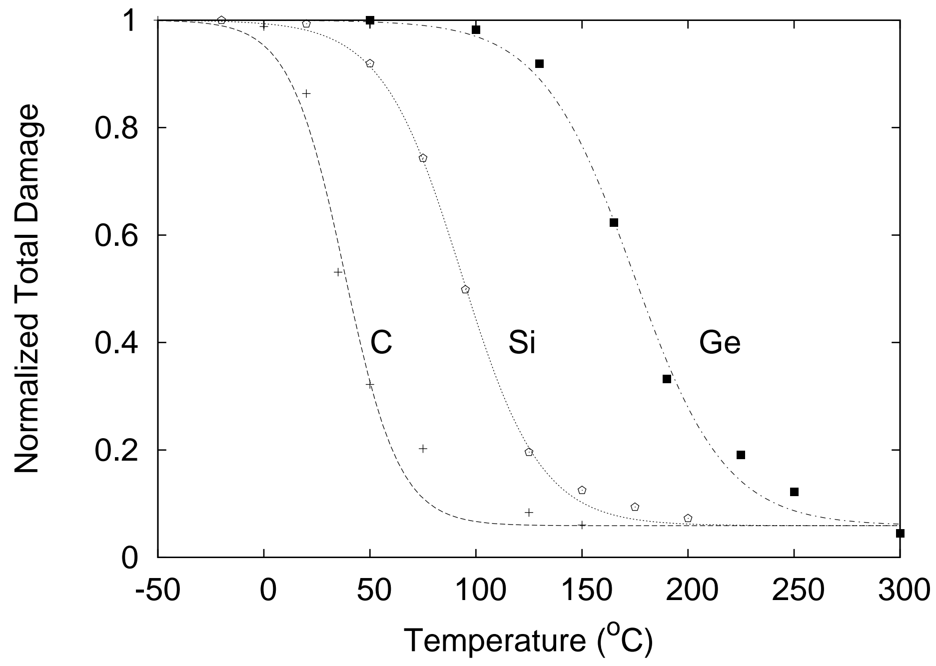

FIG. 3: